

CRACK GROWTH RESISTANCE IN CORTICAL BONE: CONCEPT OF MICROCRACK TOUGHENING

D. Vashishth, J. C. Behiri and W. Bonfield

Interdisciplinary Research Centre in Biomedical Materials, Queen Mary and Westfield College,
University of London, Mile End Road, London E1 4 NS, U.K.

Abstract—The role of microcracking in cortical bone as a toughening mechanism has been investigated in conjunction with the variation in fracture toughness with crack length. Fracture toughness tests were conducted on miniaturised compact tension specimens made from human and bovine cortical bone and the resultant microstructural damage, present in the form of microcracking on the surface, was analysed around the main propagating crack. It was found that the fracture toughness (K_{Ic}) and the cumulative number of microcracks increased linearly with crack extension in human and bovine cortical bone, although both K_{Ic} and number of microcracks were considerably higher in the latter case.

Based on these results, a mechanism, derived from the resistance (R) curve concept developed for microcracking brittle solids, is proposed to explain the fracture of cortical bone, with microcracking distributed between a frontal process zone and a significant process zone wake. Evidence to support this mechanism is given from the existing bone literature, detailed scanning electron microscopical observations and the distribution of microcracks in the process zone wake. © 1997 Elsevier Science Ltd

Keywords: Fracture toughness; Cortical bone; Microcrack; Frontal process zone; R -curve.

INTRODUCTION

Fracture in quasi-brittle materials occurs from the formation of microcracks. Loading results in the formation of a microcrack zone, referred to as the frontal process zone, around an introduced precrack. The frontal process zone develops into a process zone wake with crack propagation and the material eventually fractures (Evans and Faber, 1984). This material behaviour results in the irreversible nature of a non-linear stress/strain curve and is demonstrated by the increase in the fracture resistance as the crack advances (Hübner and Jillek, 1977; Kneehens and Steinbrech, 1982). Although cortical bone is a semi-brittle solid (Behiri and Bonfield, 1984), little is known about the onset and growth of cracks, unlike the general understanding of these processes in brittle materials.

Early studies on the fracture of bone used the strength-of-materials approach. Tensile tests indicated that loading past the yield point produced almost a flat stress/strain curve which curved upwards prior to fracture (Burstein *et al.*, 1973). These results were interpreted in terms of the two-phase model of bone in which the applied load was described as being shared between the bone mineral and the collagen (Bonfield and Li, 1967; Currey, 1964).

In parallel research, the concept of fracture toughness was introduced to bone which offered the advantage of introducing a controlled crack in bone specimens of standardised geometry to study the fracture characteristics of bone. Fracture toughness is a measure of the

inherent resistance of a material to crack extension and can be evaluated from a precracked specimen, assuming linear elastic fracture mechanics, in terms of the critical stress intensity factor, K_{Ic} , and the critical strain energy release rate, G_c . Melvin and Evans (1973) and Bonfield and Datta (1976) utilised single-edge-notched specimens to report K_{Ic} and G_c for cortical bone. Later, Wright and Hayes (1977) introduced the compact tension specimen. The advantages of using the CT specimen were that the constraints of linear elastic fracture mechanics could be more easily met and the crack propagated in a controlled manner.

In an independent approach, experiments using the compact tension specimen geometry were also performed by Bonfield *et al.* (1978), but instead of using the fracture initiation load as Wright and Hayes (1977), Bonfield *et al.* continuously monitored the load associated with an instantaneous crack length. Charalambides (1984) extended this work to investigate the effect of specimen width (W) on K_{Ic} in an attempt to extend the concept of compact tension testing from bovine to human bone. Thinner cortices and greater curvature restrict the size of compact tension specimens in human bone. Charalambides (1984) found that a wider range of a/W (crack length/width) resulted in an increase in K_{Ic} with crack length.

More recently, Norman *et al.* (1995) have also reported K_{Ic} and G_c values for human cortical bone and found that absolute values of K_{Ic} and G_c for human bone were lower than those for bovine bone. However, when normalised for their respective strengths, the two types of bone were equally tough, implying that the mechanisms which give higher strength may also be responsible for higher toughness.

Potential strengthening mechanisms in cortical bone have been described by Burstein *et al.* (1975) and Wright *et al.* (1981), who suggest microcracking as a possible

Received in final form 24 December 1996.

Address correspondence to: D. Vashishth, Interdisciplinary Research Centre in Biomedical Materials, Queen Mary and Westfield College, University of London, Mile End Road, London E1 4 NS, U.K.

mode of deformation which, according to Zioupos and Currey (1994) and Zioupos *et al.* (1994), strengthens the cortical bone. It is likely that the formation of microcracks would also toughen the bone, but no studies have been performed to investigate this phenomenon. Fracture initiation data from single-edge-notched samples have been analysed by Lakes *et al.* (1990) to explain the higher absolute toughness evaluated from notched samples. The conclusions suggest a strain-redistribution phenomenon, other than the plastic zone or the stress concentration effects, as the reason for the higher toughness. Microcracks present in the vicinity of the crack tip can cause such a effect which would consequently increase the toughness. Moreover, test data from Charalambides (1984) and Norman *et al.* (1995) show an increase in K_c with crack length, which in some quasi-brittle materials has been previously associated with microcracking and toughening (Hübner and Jillek, 1977; Knehs and Steinbrech, 1982).

Hence, the purpose of this study is to investigate if the mechanism of toughening by microcracks, common to quasi-brittle materials, occurs in cortical bone. Furthermore, as this investigation involves the determination of the influence of microcracks on a propagating crack, a secondary purpose of this study is to identify the mechanism of fracture in cortical bone. It is worth noting that, in spite of a number of studies on fracture of cortical bone, no information on the mechanisms of fracture exists in the literature.

EXPERIMENTAL PROCEDURE

Young bovine and adult human tibiae with no history of bone diseases (age in years/Sex: 36/M, 55/M, 59/M and 65/F) were obtained and frozen at -20°C with soft tissue attachments. The mid-diaphysis of the tibiae were subsequently cleaned and machined into 24 miniaturised compact tension specimens, with dimensions shown in Fig. 1, using the procedure described by Behiri and Bonfield (1980).

After machining, eight specimens [four human (59/M) and four bovine] were tested, while irrigated in Ringer's solution, on an MTS servo-hydraulic testing machine (Model 858), at an actuator speed of 0.05 mm min^{-1} at $22 \pm 1^\circ\text{C}$, and the remaining 16 specimens were treated as control samples for scanning electron microscopic (SEM) analysis only. For testing, a crack propagation gauge (MM: TK-09-CPB02) was mounted on each specimen to monitor the crack length, and the main crack, propagating in the longitudinal direction, was stopped at the end of the gauge. This procedure ensured that the damage produced in the form of microcracking was due to loading only. The complete fracture of the specimens into two parts would have caused additional damage.

Load (P), deformation (d) and crack gauge data were acquired during the test and K_c , corresponding to individual crack length (a), was calculated using (ASTM E 399-83, 1992)

$$K_c = \frac{PY_2}{BW^{0.5}}, \quad (1)$$

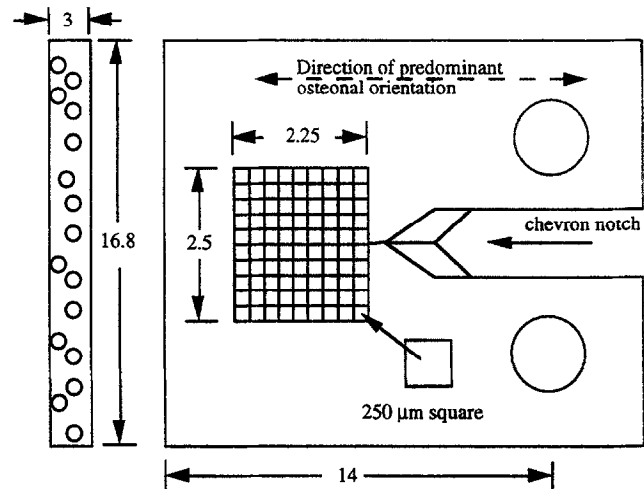


Fig. 1. Schematic diagram of compact tension specimen used to propagate crack in the longitudinal direction (parallel to the long bone axis) (all dimensions in mm). Surface area of interest (not drawn to scale) investigated under scanning electron microscope for occurrence of microcracks and the direction of predominant osteonal orientation are also shown. Circles in the side view represent osteons.

where B is the specimen thickness, W the width and Y_2 the shape function. Y_2 is defined as (Srawley, 1976)

$$Y_2 = \frac{(2 + a/W)}{(1 - a/W)^{3/2}} \{0.866 + 4.64(a/W) - 13.36(a/W)^2 + 14.72(a/W)^3 - 5.6(a/W)^4\},$$

where $0.2 \leq (a/W) \leq 1.0$.

Following testing, the specimens were analysed under the scanning electron microscope for microcracks.

POST-TESTING ANALYSIS

A part of the crack propagation gauge (2 mm) was removed from either side of the main crack for all tested specimens using tetrahydrofurane. Out of 16 control specimens, eight specimens [four human (59/M) and four bovine] were also gauged and treated in a similar manner to include any artefactual microcracks produced due to the gauge removal procedure. The remaining control specimens [four human (36/M (2) and 65/F (2)) and four bovine] were left ungauged and were not treated with tetrahydrofurane to segregate and identify the magnitude and nature of any additional microcracks produced by gauge installation and removal process. All specimens were then dehydrated in ascending series of ethanol and a vacuum at room temperature and prepared for viewing under SEM (JOEL 6300 and 6300F).

Under the SEM, a surface area of interest ($2.25 \times 2.5\text{ mm}$) was defined around the main crack and sub-divided into 90 zones based on the crack length and the distance from the main crack (Fig. 1). Each zone ($250\text{ }\mu\text{m}$ square) was then viewed under the SEM for the presence of microcracks. Microcracks were counted at $250\times$ and verified at $500\times$ and were defined to have a length $> 100\text{ }\mu\text{m}$, but $< 250\text{ }\mu\text{m}$. Microcracks $> 250\text{ }\mu\text{m}$ in length were treated as two separate microcracks. The minimum length requirement helped to

distinguish the loading cracks from dehydration and other artefactual microcracks which were generally found to be less than $100\text{ }\mu\text{m}$ in both categories of control samples (Fig. 2), while the maximum length criteria were essential to include the full contribution of longer microcracks towards the local variation in toughness which was calculated in increments of $250\text{ }\mu\text{m}$. It should be noted microcracks $>250\text{ }\mu\text{m}$ in length had their start and end points separated by a length which was greater than the increments in which the toughness was measured.

Furthermore, if one is to assign any physical meaning to the microcracks quantified by the minimum and maximum length criteria in terms of bone microstructure, they are of the order of Haversian systems or osteons ($150\text{--}250\text{ }\mu\text{m}$) which have been considered as the 'structural elements responsible for the toughness of bone' (Lakes *et al.*, 1990). A number of previous studies have either hypothesised or shown that microcracks tend to originate around osteons due to debonding at the osteon-matrix interface or osteon pull-out (Behiri and Bonfield, 1980; Carter and Hayes, 1977; Martin and Burr, 1982; Piekarski, 1970).

Following quantification of microcracks, the surface area of interest and the crack tip were photographed to assess the mechanisms of fracture.

RESULTS

Tested vs control specimens

Microcracks were counted in all the tested and control specimens. It was found that in bovine bone the tested specimens had 39.6 (S.D. = 10.6) microcracks mm^{-2} as compared to 5.4 (S.D. = 0.89) microcracks mm^{-2} in the control specimens with gauge installation and removal and 4.09 (S.D. = 1.36) microcracks mm^{-2} in the control specimens without gauge installation and removal. In contrast, in human bone, tested specimens had 11.1 (S.D. = 1.83) microcracks mm^{-2} compared to 2.3 (S.D. = 0.62) microcracks mm^{-2} in control specimens with gauge installation and removal and 2.04 (S.D. = 0.97) microcracks mm^{-2} in the control specimens without gauge installation and removal. Statistical analysis of the data indicated that the differences between tested and each category of control specimens were significant at $p < 0.01$ (ANOVA) for both human and bovine bone specimens. The difference between the two categories of control specimens (with and without gauge installation and removal), however, was non-significant for human and bovine bone specimens.

Variations in the number of microcracks and K_{c} with crack extension

For each tested specimen values of K_{c} were calculated for individual crack length (a) using equation (1) and were plotted against crack extension (da). The number of microcracks in 10 vertical zones were added up for individual crack length and were also plotted against the crack extension. Results for all human and bovine bone specimens indicate a linear increase in K_{c} and cumulative number of microcracks with crack extension (Fig. 3). It can be seen that K_{c} values for bovine bone were significantly higher than those in human bone ($p < 0.01$; ANOVA). In bovine bone, K_{c} ranged from 3.9 to $7.2\text{ MN m}^{-3/2}$ compared to 1.6 to $2.5\text{ MN m}^{-3/2}$ in human bone. Furthermore, the total number of microcracks in bovine bone were also found to be significantly higher than in human bone ($p < 0.01$; ANOVA).

Mechanisms of fracture

SEM micrographs of crack propagation are shown in Figs 4 and 5. Figure 4(a) shows the crack propagation in a typical bovine bone specimen. It can be seen that two cracks initially grew out of the chevron notch, but only one continued to become the main crack (1). The main crack then follows a tortuous route (2) until it is stopped (3). The presence of frontal process zone is apparent in (3), which is shown at higher magnifications in Fig. 4(b). Similar micrographs of human bone are shown in Fig. 5.

The process zone wake for bovine and human bone can be seen in the Figs 4(a) and 5(a), respectively. The distribution of the microcracks in the wake is presented in Fig. 6. It can be seen that microcrack density remains almost constant with the increase in the normal distance from the fracture plane for both human and bovine bone and that, as noted above, it is higher for the bovine bone.

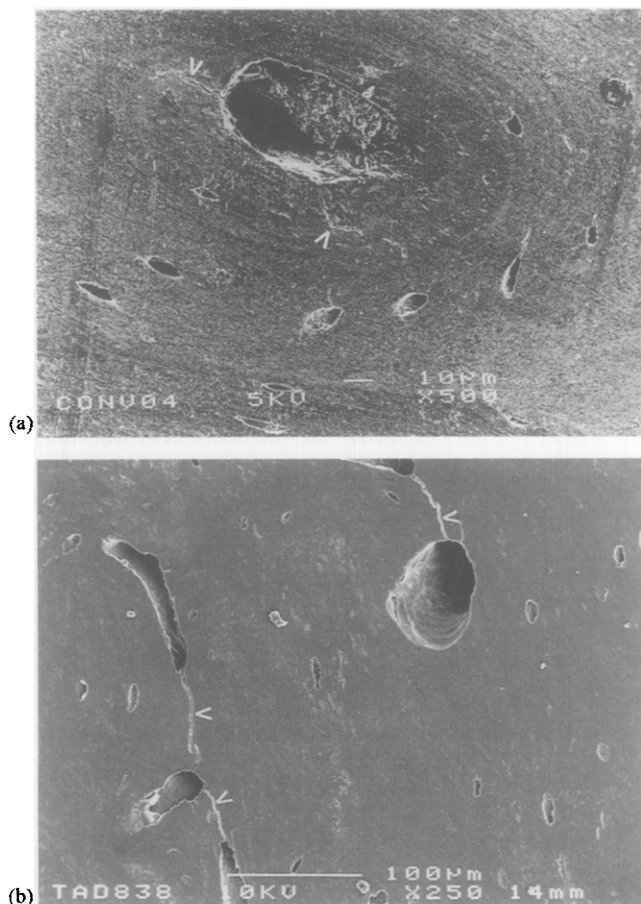


Fig. 2. Typical surfaces of a bovine bone control specimen (a) with gauge installation and removal and (b) without gauge installation and removal showing artefactual microcracks $<100\text{ }\mu\text{m}$.

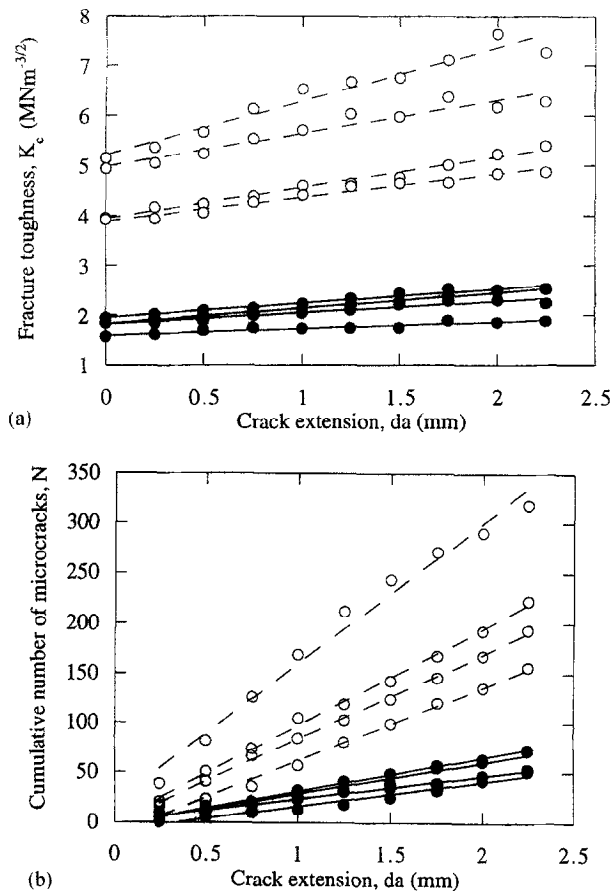


Fig. 3. Variation of (a) fracture toughness (K_c) and (b) cumulative number of microcracks (N) with crack extension for four human bone and four bovine bone specimens. Hollow and solid circles indicate bovine and human bone specimens, respectively. Each line represents one specimen. Correlation coefficients of linear regression (R) for bovine bone specimens (Top line to bottom line) K_c : 0.97, 0.96, 0.99 and 0.98; Cumulative number of microcracks: 0.99, 0.99, 0.99 and 0.99. Correlation coefficients of linear regression (R) for human bone specimens (top to bottom line) K_c : 0.98, 0.99, 0.96 and 0.94; Cumulative number of microcracks: 0.99, 0.98, 0.99 and 0.98. Note that statistical test (ANOVA) indicated that initial crack lengths of human and bovine bone specimens were not significantly different and hence crack length data have been converted and represented as crack extension data in this figure.

DISCUSSION

In this study the role of microcracks in toughening cortical bone was investigated. Toughening was demonstrated by fracture toughness tests conducted on human and bovine cortical bone, both of which showed a linear increase in the values of K_c and cumulative number of microcracks with crack propagation (Fig. 3). It was also demonstrated that a majority of these microcracks were produced as a result of loading, as both categories of control specimens (with and without gauge installation and removal) showed minimal artefactual damage. Furthermore, consistent with the toughening mechanisms in quasi-brittle microcracking solids, the presence of a frontal process zone and a significant process zone wake were noted in the scanning electron micrographs of human and bovine cortical bone (Figs 4 and 5). The distribution of microcracks in the process zone wake was, however, different. The microcrack density remained almost con-

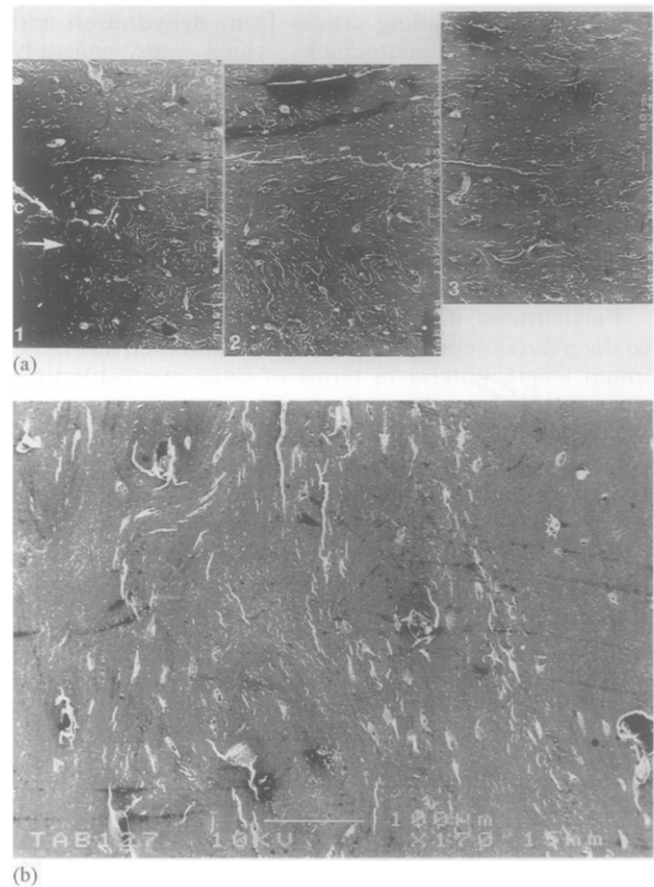


Fig. 4. (a) Crack propagation in a typical bovine bone compact tension specimen (Stages 1-3). Note that the position of the chevron notch is shown by the letter 'c' in Stage (1) and the direction of predominant osteonal orientation is shown by an arrow. (b) Higher magnification photomicrograph of frontal process zone shown in Stage (3). Note that the photomicrograph in (b) has been rotated by 90 degrees (clockwise) with respect to (a).

stant with the increase in the normal distance from the fracture plane for both human and bovine bone (Fig. 6) and did not show the decline common to engineering materials.

These results support the concept of microcrack toughening in cortical bone and also highlight, for the first time, the presence of a unique mechanism of fracture in bone.

The increase in K_c and cumulative number of microcracks with crack extension are consistent with a previous study of Charalambides (1984) and additional evidence regarding the increase in K_c with crack extension comes from Norman *et al.* (1995). Figure 7 shows a comparison between the present and three previous studies. A marked increase in K_c with a/W is apparent in all studies, with the exception of Behiri and Bonfield (1984). It should be noted that Behiri and Bonfield (1984) used considerably wider specimens ($W = 26$ mm) to obtain plane strain conditions at the crack tip and subsequent work of Bonfield *et al.* (1985) has shown that fracture toughness characteristics are considerably affected by width. Hence, K_c versus crack length data from the other studies cannot be directly compared with the Behiri and Bonfield investigation.

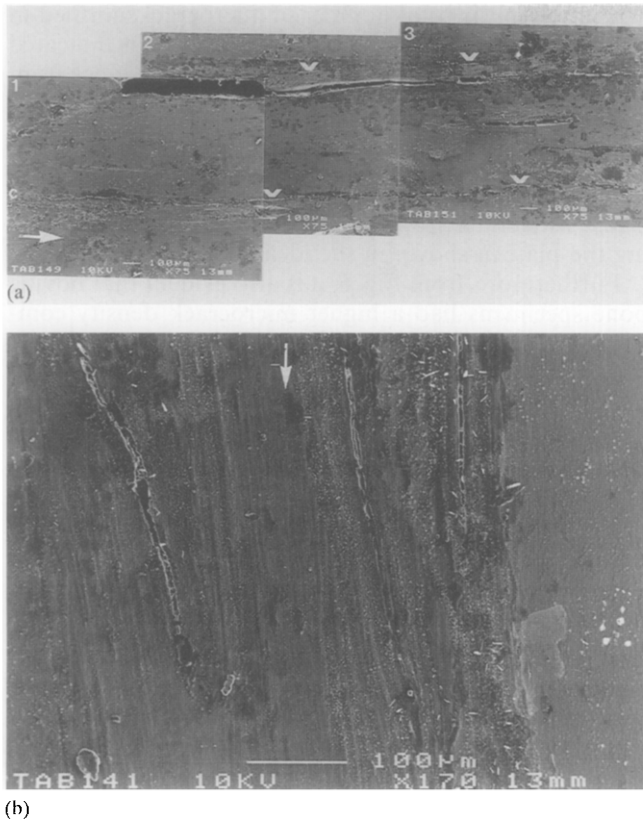


Fig. 5. (a) Crack propagation in a typical human compact tension specimen (Stages 1–3). The position of the chevron notch is shown by the letter 'c' in Stage (1) and the direction of predominant osteonal orientation is shown an arrow. The letter 'v' in Stages (2) and (3) indicates the microcracks in the process zone wake. (b) Higher magnification photomicrograph of frontal process zone shown in Stage (3). Note that the photomicrograph in (b) has been rotated 90 degrees (clockwise) with respect to (a) and that compared to Fig. 4, microcracks in human bone tend to occur along the predominant osteonal direction.

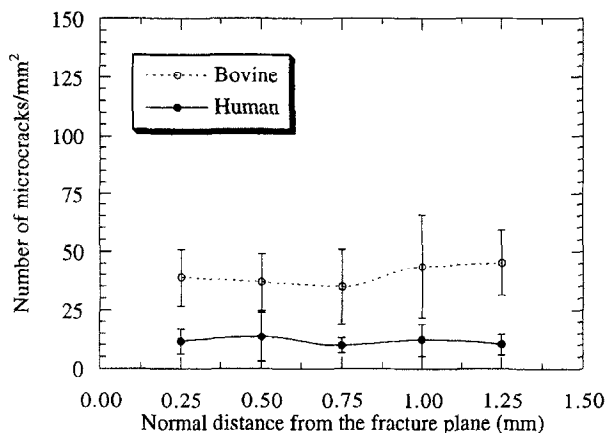


Fig. 6. Distribution of microcracks around the main crack in human and bovine bone compact tension specimens.

An increase in K_{Ic} with the crack extension can be explained by the R or resistance curve concept. According to ASTM E 561-86 (1992), an R -curve is a plot of the crack extension force versus the crack extension, for slow-stable crack propagation, and it describes the toughness development in a material. In engineering lit-

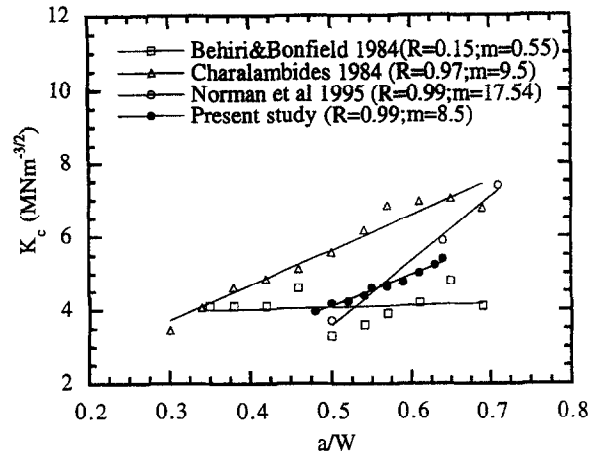


Fig. 7. Comparison of bovine bone fracture toughness data obtained in the present study with the previous investigations. In the figure ' R ' indicates the correlation coefficient and ' m ' indicates the slope.

erature the terms 'crack extension force' or 'crack growth resistance' are generally used instead of 'fracture toughness', to emphasize its variation with the crack length, but for consistency with the previous bone literature the term 'fracture toughness' is retained in this investigation.

The significance of the R -curve is that its shape, depending on the conditions (plane strain or stress), can be used to predict material behaviour and fracture mechanisms. Brittle materials demonstrate a flat R -curve. Loading results in an increase in stress around a pre-existing flaw, which produces unsteady crack propagation and failure once the critical value is reached. In contrast, ductile materials undergo stable crack propagation due to the formation of a plastic zone around the crack tip. The plastic zone grows as the crack advances and thereby absorbs part of the energy available at the crack tip for extension. This effect increases the toughness of the material and results in a rising R -curve (Anderson, 1990).

A rising R -curve, however, is not just a characteristic of ductile materials and can even be achieved in brittle materials such as ceramics (Kneehens and Steinbrech, 1982; Hübner and Jillek, 1977). A model to explain this behaviour was presented by Evans and Faber (1984), in which the development of the fracture from a frontal process zone to a wake was described to explain the rising R -curve (Fig. 8). It was shown that toughening effects were mainly produced by the microcracks formed in the wake as their formation results in the residual opening and the associated dilation of the crack tip. This effect, in turn, causes a redistribution of stresses in the crack-tip region (Hutchinson, 1987), which eventually reduces the crack extension force, increases the toughness of the material and results in a rising R -curve.

Hence, based on the increase in K_{Ic} with crack extension which is in the form of an R -curve [Fig. 3(a)], it is proposed that a similar mechanism of fracture involving microcrack toughening occurs in cortical bone. Evidence in support of this mechanism is given in terms of the existing bone literature, detailed SEM observations and the distribution of microcracks.

For cortical bone to behave in the above manner, it should, at least at some level, resemble microcracking

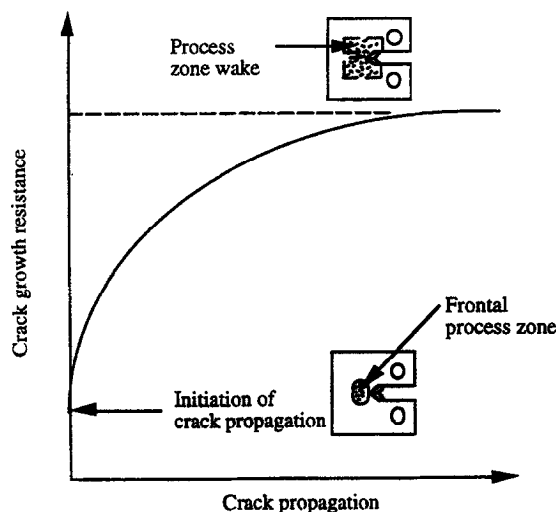


Fig. 8. Schematic illustration of *R*-curve effects in microcracking brittle solids. Development of fracture from frontal process zone to process zone wake is also shown (redrawn from Evans and Faber, 1984).

quasi-brittle solids. Evidence from the bone literature shows that a number of previous studies have implicated the bone mineral in fracture or deformation of bone (Bonfield and Li, 1966; Burstein *et al.*, 1975; Wright *et al.*, 1981). Although controversy still exists about the arrangement of hydroxyapatite crystals within the collagen, the accepted arrangement includes a parallel stacking of the plate-like mineral within portions of contiguous and adjacent hole zones in the collagen array (Christoffersen and Landis, 1991). It has been suggested that mineral present in adjacent collagen molecules may be linked to form plates which can extend through a number of collagen microfibrils (Weiner and Traub, 1992). Such a structure, when loaded, is bound to be influenced by bone mineral, and Currey, in a number of studies (1979, 1984, 1989), has shown this to be true. Therefore, it is likely that bone mineral, which is the ceramic content of bone, plays a determining part in the fracture mechanism. Moreover, the stress/strain curves from cortical bone (Burstein *et al.*, 1973) show a striking resemblance with the stress/strain curve obtained for brittle microcracking solids (Evans and Fu, 1985) and the origin of a rising *R*-curve is manifested in such a curve (Evans and Faber, 1984), given the information that cortical bone is a semi-brittle material (Behiri and Bonfield, 1984) and that it undergoes microcracking when loaded in the post yield region (Zioupos and Currey 1994, Zioupos *et al.* 1994).

More direct evidence in support of the proposed mechanism comes from Figs 4–6, in which the presence of the frontal process zone and the distribution of the microcracks in the wake are shown. The frontal process zone in bovine bone [Fig. 4(b)] is contained within a cone. Human bone, however, shows a different configuration, in which three parallel cracks represent the frontal process zone [Fig. 5(b)]. Figure 6 shows the distribution of microcracks produced in a wake. From the graph it appears that the microcrack density remains approximately constant with the increase in the normal distance from the fracture plane. This finding suggests that the

saturation in the total number of microcracks formed in the wake, common to certain ceramics, which is indicated by a decrease in the crack density with the distance from the main crack (Rühle, 1988; Zhonghua *et al.*, 1993), has not been achieved. It is for this reason that the *R*-curves as well as the cumulative number of microcracks for human and bovine bone show a continuous linear increase with crack propagation (Fig. 3) rather than achieving the plateau shown in the idealised curve in Fig. 8.

Furthermore, from Fig. 6, it is also evident that bovine bone specimens had a higher microcrack density compared to human bone specimens. This, in turn, reflects the capability of bovine cortical bone to form more microcracks during crack propagation as compared to human cortical bone. The more microcracks a material can form, the tougher it becomes and a comparison of K_{IC} values between human bone ($1.6\text{--}2.5\text{ MN m}^{-3/2}$) and bovine bone ($3.9\text{--}7.2\text{ MN m}^{-3/2}$) suggests that this indeed is the case.

Acknowledgements—This work has been funded by the IRC programme grant received from the Engineering and Physical Sciences Research Council. The authors are grateful to Dr Z. Luklinska for her help with the scanning electron microscopy and to Dr H. Schechtman and Dr K.E. Tanner for helpful discussions. Thanks are also due to Mr M. Elliot and Mr J. Trifonas for their assistance with the machining and experimentation.

REFERENCES

- Anderson, T. L. (1990) *Fracture Mechanics: Fundamental and Applications*. CRC Press, Boca Raton, FL.
- ASTM E 399-83 (1992) Standard test method for plane strain fracture toughness testing of metallic materials. *ASTM Annual Book of Standards*, Section 2. pp. 480–503.
- ASTM E 561-86 (1992) Standard practice for *R*-curve determination. *ASTM Annual Book of Standards*.
- Behiri, J. C. and Bonfield, W. (1980) Crack velocity dependence of longitudinal fracture in bone. *Journal of Materials Science* **15**, 1841–1849.
- Behiri, J. C. and Bonfield, W. (1984) Fracture mechanics of bone—the effects of density, specimen thickness and crack velocity on longitudinal fracture. *Journal of Biomechanics* **17**, 25–34.
- Bonfield, W., Behiri, J. C. and Charalambides, B. (1985) Orientation and age related dependence of the fracture toughness on cortical bone. In *Biomechanics: Current Interdisciplinary Research*, eds S. M. Perren and E. Schneider, pp. 185–189. Martinus Nijhoff, Dordrecht.
- Bonfield, W. and Datta, P. K. (1976) Fracture toughness of compact bone. *Journal of Biomechanics* **9**, 131–134.
- Bonfield, W., Grynblas, M. D. and Young, R. J. (1978) Crack velocity and the fracture of bone. *Journal of Biomechanics* **11**, 473–479.
- Bonfield, W. and Li, C. H. (1967) Anisotropy of nonelastic flow in bone. *Journal of Applied Physics* **38**, 2450–2455.
- Burstein, A. H., Reilly, D. T. and Frankel, V. H. (1973) Failure characteristics of bone and bone tissue. In *Perspectives in Biomedical Engineering*, ed. R. M. Kenedi, pp. 131–134. Macmillan Press, Glasgow.
- Burstein, A. H., Zika, J. M., Heiple, K. G. and Klein, L. (1975) Contribution of collagen and mineral to the elastic-plastic properties of bone. *Journal of Bone and Joint Surgery* **57A**, 956–961.
- Carter, D. R. and Hayes, W. C. (1977) Compact bone fatigue damage: A microscopic examination. *Clinical Orthopaedics and Related Research* **127**, 265–274.
- Charalambides, B. (1984) Fracture toughness of cortical bone – effect of specimen geometry. M. Phil. thesis, University of London.
- Christoffersen, J. and Landis, W. J. (1991) A contribution with review to the description of mineralization of bone and other calcified tissues *in vivo*. *Anatomy Rec.* **230**, 435–450.
- Currey, J. D. (1964) Three analogies to explain the mechanical properties of bone. *Biorheology* **2**, 1–10.
- Currey, J. D. (1979) Mechanical properties of bone tissue with greatly differing functions. *Journal of Biomechanics* **12**, 313–319.

- Currey, J. D. (1984) *The Mechanical Adaptations of Bones*. Princeton University Press, Princeton, NJ.
- Currey, J. D. (1989) Strain rate dependence of the mechanical properties of reindeer antler and the cumulative damage model of bone fracture. *Journal of Biomechanics* **22**, 469–475.
- Evans, A. G. and Faber, K. T. (1984) Crack growth resistance of microcracking brittle materials. *Journal of American Ceramic Society* **67**, 255–260.
- Evans, A. G. and Fu, Y. (1985) Some effects of microcracks on the mechanical properties of brittle solids-II: Microcrack toughening. *Acta Metallurgica* **33**, 1525–1531.
- Hübner, H. and Jillek, W. (1977) Sub critical crack extension and crack resistance in polycrystalline alumina. *Journal of Materials Science* **12**, 117–125.
- Hutchinson, J. W. (1987) Crack tip shielding by microcracking in brittle solids. *Acta Metallurgica* **35**, 1605–1619.
- Knehans, R. and Steinbrech, R. (1982) Memory effect of crack resistance during slow crack growth in notched Al_2O_3 bend specimens. *Journal of Materials Science Letters* **1**, 327–329.
- Lakes, R. S., Nakamura, S., Behiri, J. C. and Bonfield, W. (1990) Fracture mechanics of bone with short cracks. *Journal of Biomechanics* **23**, 967–975.
- Martin, R. B. and Burr, D. (1982) A hypothetical mechanism for the simulation of osteonal remodelling by fatigue damage. *Journal of Biomechanics* **15**, 137–139.
- Melvin, J. W. and Evans, F. G. (1973) Crack propagation in bone. In *Biomaterials Symposium AMD*, eds Y. C. Fung, and J. A. Brighton, Vol. 2, pp. 87–88. American Society of Mechanical Engineers, New York.
- Norman, T. L., Vashishth, D. and Burr, D. B. (1995) Fracture toughness of human bone under tension. *Journal of Biomechanics* **28**, 309–320.
- Piekarski, K. (1970) Fracture of bone. *Journal of Applied Physics* **41**, 215–223.
- Rühle, M. (1988) Microcrack and transformation toughening of zirconia-containing alumina. *Material Science Engineering* **A105/106**, 77–82.
- Srawley, J. E. (1976) Wide range stress intensity factor expression for ASTM E 399 standard fracture toughness specimens. *International Journal of Fracture Mechanics* **12**, 475.
- Weiner, S. and Traub, W. (1992) Bone structure: from ångströms to microns. *The FASEB Journal* **6**, 879–885.
- Wright, T. M. and Hayes, W. C. (1977) Fracture mechanics parameters of compact bone – Effects of density and specimen thickness. *Journal of Biomechanics* **10**, 419–430.
- Wright, T. M., Vosburgh, F. and Burstein, A. H. (1981) Permanent deformation of compact bone monitored by acoustic emission. *Journal of Biomechanics* **14**, 405–409.
- Zhonghua, L., Yong, Z. and Schmauder, S. (1993) A cohesion model of microcrack toughening. *Engineering Fracture Mechanics* **44**, 257–265.
- Zioupou, P. and Currey, J. D. (1994) The extent of microcracking and morphology of microcracks in damaged bone. *Journal of Materials Science* **29**, 978–986.
- Zioupou, P., Currey, J. D. and Sedman, A. J. (1994) An examination of the micromechanics of failure of bone and antler by acoustic emission tests and laser scanning confocal microscopy. *Medical Engineering and Physics* **16**, 203–212.